

# Centrifuge model tests on long-term consolidation of clay ground after earthquakes and negative impact against seismic behavior of upper liquefiable sand caused by clay ground

Koichi Isobe<sup>1</sup>, Y. Hatanaka<sup>1</sup>, and K. Tomisawa<sup>2</sup>

<sup>1</sup> Division of Field Engineering for Environment, Hokkaido University, Kita 13, Nishi 8, Kita-ku, Sapporo 060-8628, Japan.

<sup>2</sup> Civil Engineering Research Institute for Cold Region, 1-3-1-34, Hiragishi, Toyohira-ku, Sapporo 062-8602, Japan.

## ABSTRACT

In this paper, the following two kinds of mechanism has been investigated based on shaking model tests under centrifugal acceleration of 50 G; a) long-term consolidation of clay ground after earthquakes and b) seismic behavior of liquefiable sand resting on clay ground. The results for a) series of tests show the structured clay has higher initial stiffness and liquefaction strength than the poorly-structured clay, but the highly-structured clay is more brittle than the poorly-structured clay. From the results for b) series of tests, it is confirmed that the response acceleration of the clay is largely amplified, resulting in the liquefaction of sand resting on clay ground at the earlier stage.

**Keywords:** clay; liquefaction; consolidation; shaking table tests; centrifuge model tests

## 1 INTRODUCTION

After the Niigata Prefecture Chuetsu-Oki Earthquake of 2007, long-term settlement of clay was observed in Kashiwazaki city. The ground investigation has revealed an existence of structured alluvial clay deposit in this city. It is said that this kind of settlement is caused by collapse of structured clay (Isobe & Ohtsuka, 2013). Also, the liquefaction damages have been observed over a wide area in the Urayasu district in Chiba Prefecture due to the 2011 off the Pacific coast of Tohoku Earthquake, where an alluvial clay layer is deposited under the liquefiable sand layer. It is reported that the sea side where the clay layer thickness is thicker is more damaged. Therefore, it is pointed out that the presence of soft clay may multiply ground disasters although it is generally regarded that clay is not liquefiable.

In this paper, the following two kinds of mechanism has been investigated; a) long-term consolidation of clay ground after earthquakes and b) seismic behavior of liquefiable sand resting on clay ground.

## 2 EXPERIMENT OUTLINES

### 2.1 Model grounds and their properties

Fig.1 shows test condition and cases. Case1 and 2 are conducted to clarify long-term consolidation mechanism of clay ground after earthquakes using highly-structured clay. Case3 and 4 are conducted to investigate seismic behavior of liquefiable sand resting on clay ground, varying the thickness of clay ground.

Kaolin clay ( $\rho_s = 2.63$  (g/cm<sup>3</sup>),  $W_L = 43.50$  (%),  $W_p$

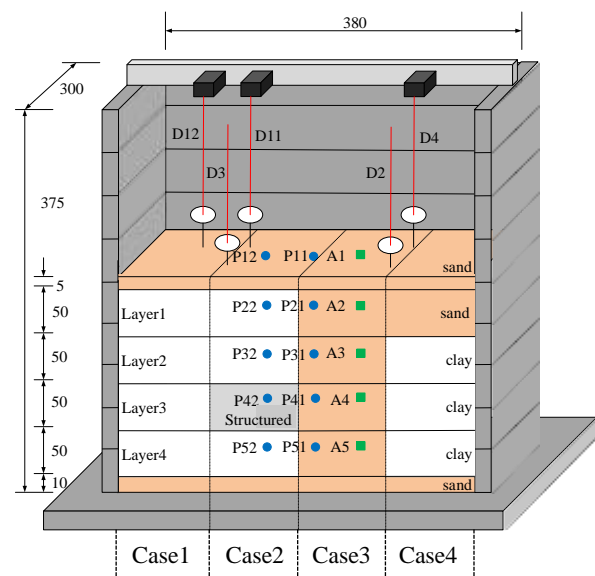


Fig. 1. Model grounds in model type scale (unit: mm), P: Pore water pressure gauge, A: Accelerometer, D: Displacement gauge.

$= 28.12$  (%),  $I_p = 15.38$  (%)) was used, adding an ordinary Portland cement with dry mass ratio of 0.5% to the clay to simulate structured clay ground. Higher degree of structured clay ground was made curing for 3 days, and less degree of structured ground was made by remixing and reconsolidating after cured for 28 days more. As shown in Fig. 2, void ratio of kaolin clay cured for 3 days is larger than that of reconsolidated after cured for 28 days more at the same consolidation pressure. Thus, structured clay ground can be reproduced. Undrained cyclic compression triaxial tests were conducted for above two types of specimens. The liquefaction strength of the normally consolidated

kaolin clay without cement ( $R_{L20}$ ) is 0.15. The number of cycles at double amplitude of axial strain reaches 5 % is 35 times (remixing) and 32 times (3 days). A dynamic compression index,  $C_d$ , which is defined by Eq. (1), was 0.512 (remixing) and 0.555 (3 days), respectively. It indicates that the structured clay (3 days) has higher compressibility than the less structured clay (remixing) against cyclic shear loading.

$$C_d = \frac{\Delta u}{\log SRR} = \frac{\Delta u}{\log \left( \frac{p'}{p' - \Delta u} \right)} \quad (1)$$

where,  $\Delta u$ : excess pore water pressure,  $p'$ : effective stress. More detail of the property is shown in the reference (Hatanaka & Isobe, 2018).

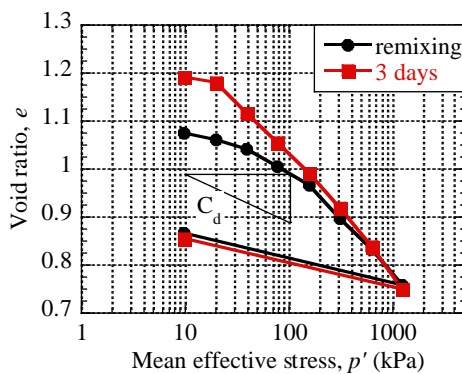


Fig. 2. Consolidation curve of Kaolin clay.

In the centrifugal model experiments, ground motions were given to the ground models with the scale of 1/50 from the ground bottom under centrifugal acceleration of 50 G. The model grounds are made in laminar boxes (40 mm  $\times$  9 stages) attaching membrane with a thickness of 0.3 mm on the inside walls, and the depth is 10 m in total with 2.5 m per one layer in prototype scale as shown in Fig. 1. The model grounds were prepared by self-weight consolidation under centrifuge acceleration of 50 G layer by layer for about an hour. The liquefiable layers were prepared by air pluviation method with silica sand No.7 ( $D_r = 70\%$ ,  $R_{L20} = 0.20$ ) and fully saturated with viscous fluid of dynamic viscosity 50 times greater than water after vacuum deaeration. Excess pore water pressure, acceleration and settlement of each layer during and after shakes were measured. The outlines of model ground and layout of instruments are shown in Fig. 1.

## 2.2 Shaking conditions and test cases

After having been stable in the centrifuge field with an acceleration of 50 G, the ground motions were generated, changing the magnitude of the input acceleration progressively after the excess pore water pressure was dissipated. The input waves used in the experiment were sine waves of 1 Hz with tapers, and the number of waves per an earthquake is 30. The target

input accelerations at each step were 50 gal, 100 gal, 150 gal and 150 gal, respectively. During and after the shakes, the surface of the ground was under drained condition, the side and bottom of the ground were under undrained condition.

Two cases were conducted in a) series of tests. For the model ground in Case 1, kaolin clay with less structure was used from Layer 1 to Layer 4. In Case 2, less structured kaolin clay is used for Layer 1, 2 and 4 in the same manner as Case 1, but high degree of structured clay cured for 3 days is used for Layer 3 to simulate the real ground in which was really damaged by Great East Japan earthquake of 2011 and Niigata-ken Chuetsu-oki Earthquake of 2007 (See Isobe and Ohtsuka, 2013). The other two cases were conducted in b) series of tests. For the model ground in Case 3, liquefiable sand layer ( $D_r = 70\%$ ,  $R_{L20} = 0.20$ ) was used from Layer 1 to Layer 4. In Case 4, less structured kaolin clay is used for Layer 2 thorough 4 in the same manner as Case 1, but Layer 1 is prepared with the liquefiable sand in the same manner as Case 3.

## 3 EXPERIMENT RESULTS

### 3.1 Long-term consolidation of clay ground after earthquakes

The time histories of response acceleration in the ground for Cases 1 and 2 are shown in Fig. 4. But, for the convenience of the space, that of 100 gal and second 150 gal are omitted. As an overall trend, the response acceleration tended to be amplified larger for the shallower ground against the small ground motions. Therefore, the seismic waves are amplified against small ground motions in the clay ground. However, the response acceleration in the surface layer (A1) sharply decreased as the input motion and response acceleration increased. In addition, the sudden reduction of the response acceleration in other upper parts of the ground was seen against the larger ground motions, and the period of the response acceleration were prolonged generating sudden reduction, resulting from decrease of the stiffness due to generating excess pore water pressure and larger shear strain.

The maximum values of response acceleration at each measurement point normalized by the input acceleration are shown in Fig. 5. As mentioned above, in both cases (Cases 1 and 2), the maximum value of the response acceleration tended to increase at the upper part of the ground when the amplitude of the input acceleration was less than 100 gal. However, the maximum value of the response acceleration decreased when the amplitude of the input acceleration was more than 100 gal for the following presumptive reasons; degradation of the stiffness of the ground due to excess pore water pressure and shear strain. In addition, the maximum value of the response acceleration of Layer 3 in Case 2 was larger than that in Case 1 for the first (50 gal) and second steps (100 gal). It means that the

seismic wave is amplified more in the high degree of structured clay ground with larger stiffness.

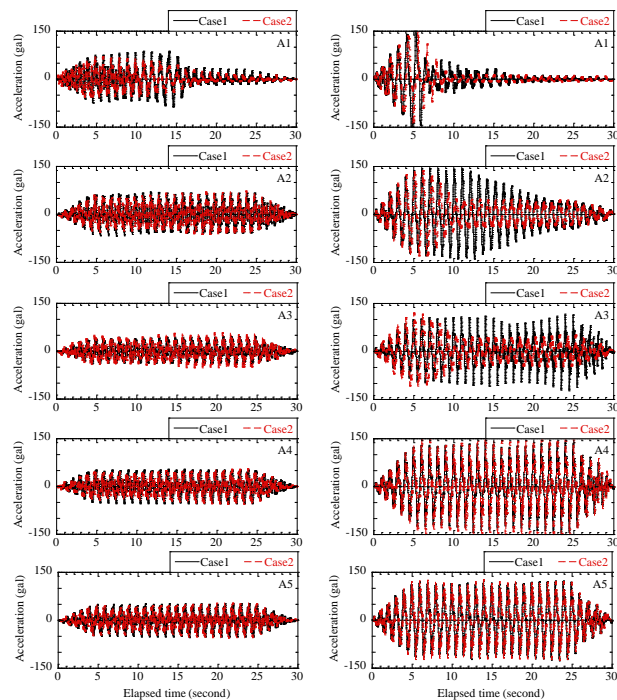


Fig. 4. Time history of the response acceleration of the ground of Cases 1 and 2 (left: 50 gal, right: 150 gal).

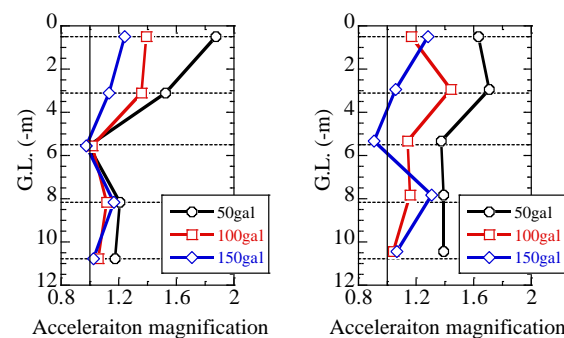


Fig. 5. Maximum values of the response acceleration normalized by input acceleration (left: Case 1, right: Case 2).

The maximum values of excess pore water pressure ratio in depth during and after shaking is shown in Fig. 6. The maximum values of excess pore water pressure ratio in Case 2 were larger than that in Case 1 for the first and second steps (50 gal and 100 gal). It is thought to be caused by the result that seismic wave is amplified more in the highly-structured clay ground. However, the excess pore water pressure ratio of both cases was almost identical for the third steps (150 gal). It can be thought that the ground for Case 2 became similar condition as Case 1 due to the deterioration of the structure against larger ground motions.

The settlement of each layer and total settlement are shown in Fig. 7. The settlement of each layer in Case 1 came to be small sequentially from the surface layer to the depth direction. However, the settlement of Layer 3

with highly-structured clay in Case 2 was relatively larger than the other layers. It is the reason why the seismic waves were amplified in highly-structured clay ground with larger shear stiffness, and then fragile behavior was observed by deterioration of structure with large shear deformation and excess pore water pressure. As a result, total settlement of Case 2 was larger than that of Case 1. It is consistent with the result that the dynamic compression index,  $C_d$  of the structured clay is larger.

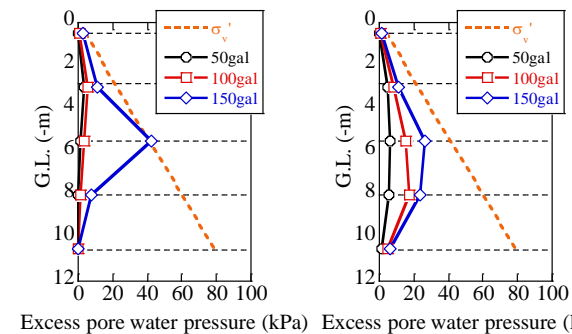


Fig. 6. Maximum values of the excess pore water pressure ratio (left: Case 1, right: Case 2).

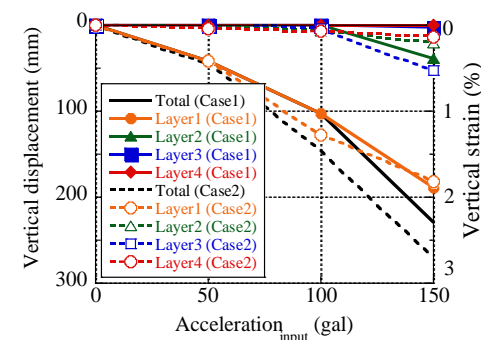


Fig. 7. Vertical displacement after each step.

### 3.2 Seismic behavior of liquefiable sand resting on clay ground

Based on the time histories of response acceleration in the ground for Cases 3 and 4, the maximum values of response acceleration at each measurement point normalized by the input acceleration are shown in Fig. 8. In both cases (Cases 3 and 4), the maximum value of the response acceleration tended to increase at the upper part of the ground when the amplitude of the input acceleration was less than 50 gal. However, the maximum value of the response acceleration decreased when the amplitude of the input acceleration was more than 50 gal for the smaller stiffness of the clay ground and the degradation of the stiffness of the clay ground due to excess pore water pressure and shear strain.

The maximum values of excess pore water pressure ratio in depth during and after shaking is shown in Fig. 9. The maximum values of excess pore water pressure ratio of the tops (P1 and P2) in Case 4 were larger than



that in Case 3 for the all steps. It is thought to be caused by the smaller stiffness of the clay ground. As a result, Layer 1 in Case 4 resting on the clay ground earlier liquefied than that in Case 3, and the response acceleration heavily damped during shaking.

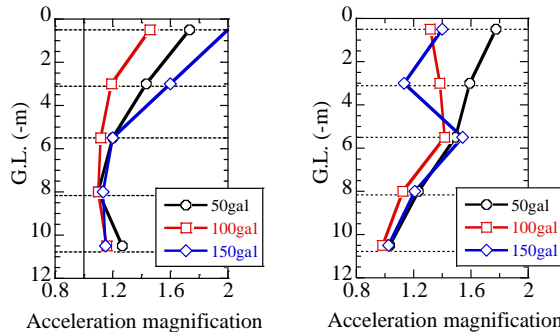


Fig. 8. Maximum values of the response acceleration normalized by input acceleration (left: Case 3, right: Case 4).

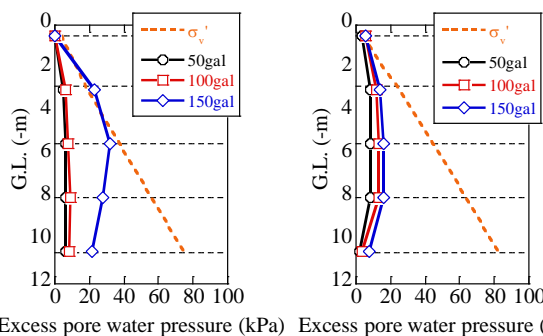


Fig. 9. Maximum values of the excess pore water pressure ratio (left: Case 3, right: Case 4).

Fig. 10 shows the relationship between shear modulus and shear strain for each layer, which is calculated based on the results of acceleration at each position (see Hatanaka and Isobe, 2018). According to these figures, the shear modulus of Layers 2 and 3 in Case 3 was kept higher than that in Case 4, resulting in the smaller shear strain of Layers 2 and 3 in Case 3 than that in Case 4. It led the liquefaction of the liquefiable

sand layer resting on clay ground occurred at the earlier stage. As a result, the reduction of shear modulus of Layer 1 in Case 4 was observed in spite of the fact that Layer 1 for both cases are same condition.

#### 4 CONCLUSIONS

The conclusions obtained in this experiment are as follows.

The structured clay has higher initial stiffness and liquefaction strength than the poorly-structured clay, but the highly-structured clay is more brittle than the poorly-structured clay, especially relating to behavior of excess pore water pressure. Also, the compression index caused by earthquakes of the highly-structured clay is higher than that of the poorly-structured clay. Thus, the settlement of structured clay after large-scale earthquakes is more serious than that of poorly-structured clay.

The response acceleration of the clay is largely amplified, comparing to the liquefiable silica sand #7 with  $D_r$  of 70% and  $R_{L20}$  of 0.20, resulting in the liquefaction of surface layer resting on clay ground at the earlier stage. It is coincident with observation in the 2011 off the Pacific coast of Tohoku Earthquake.

However, discussion based on further experiments and numerical analytical approaches are necessary to predict and evaluate negative impact for structures during earthquakes caused by clay ground since the number of the experimental cases and conditions are limited.

#### REFERENCES

- Hatanaka, Y. and Isobe, K. (2018). Seismic amplification of clay ground and long-term consolidation after earthquake. Proc., Physical Modelling in Geotechnics 1, London, 891-896.
- Isobe, K. and Ohtsuka, S. (2013). Study on long-term subsidence of soft clay due to 2007 Niigata Pre-fecture Chuetsu-Oki Earthquake. Proc., the 18th International conference on soil mechanics and geotechnical engineering 1, Paris, 1499-1502.

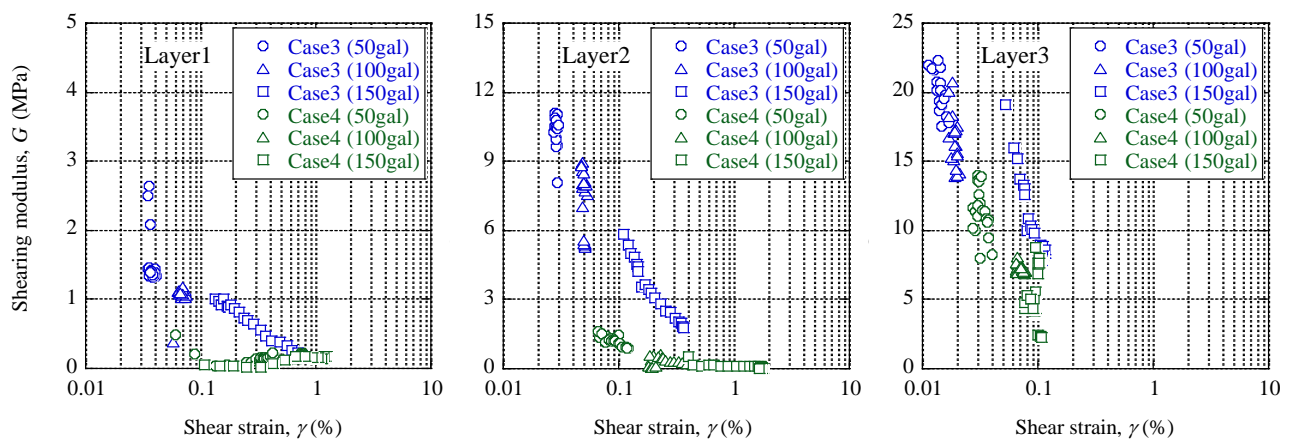


Fig. 10. Relationship between shear strain and shear modulus for Cases 3 and 4 (left: Layer1, middle: Layer 2 and right: Layer 3)